The 8th European Congress on Computational Methods in Applied Sciences and Engineering
ECCOMAS Congress 2022
5-–9 June 2022, Oslo, Norway

FLUID-STRUCTURE INTERACTION TOOL FOR MORPHING BLADES

Giada Abate[1], Johannes Riemenschneider[2]

[1] German Aerospace Center (DLR)
Institute of Composite Structures and Adaptive Systems
Lielienthalpl. 7, 38108 Braunschweig, Germany
e-mail: giada.abate@dlr.de, www.dlr.de

[2] German Aerospace Center (DLR)
Institute of Composite Structures and Adaptive Systems
Lielienthalpl. 7, 38108 Braunschweig, Germany
email: johannes.riemenschneider@dlr.de, www.dlr.de

Key words: Fluid-structure interaction, CFD, Structural analysis, Morphing, Blades, Cascade

Abstract. The design of aeronautical components commonly involves two highly coupled disciplines: aerodynamics and structural mechanics. The interaction between them becomes even more relevant when morphing aeronautical structures are studied. Considering the importance of morphing technology for the future of the aerospace industry, several tools have already been developed to couple these two disciplines together, but all of them deal with pure two-dimensional or three-dimensional aero-structural problems. In some circumstances, the study of aeronautical components requires to couple a 2D computational fluid-dynamics (CFD) analysis with a 3D finite element analysis (FEA). This usually happens in the preliminary design phase of aeronautical engine blades (i.e. compressor blades) where the aerodynamic study of the original 3D geometry is replaced by the analysis of a 2D blade cascade in order to reduce the overall computational cost. However, such an approach requires a specific method to couple the 2D CFD geometry/mesh with the 3D FEA geometry/mesh in order to transfer the aerodynamic loads from the CFD analysis to the structural one. As mentioned before, the existing fluid-structure interaction (FSI) tools cannot be implemented to solve a 2D-3D problem; therefore, a novel 2D-3D aero-structure coupling approach needs to be developed. This paper describes step-by-step the 2D-3D aero-structure coupling strategy applied to the performance analysis of a morphing blade cascade with the goal of enhancing its aerodynamic performance. The results show a relevant decrease in the total pressure losses of the morphing cascade thanks to the adapting blade leading-edge. In order to highlight the reliability of the FSI framework, the developed approach is applied to four different blade configurations which differ in size and location of the two morphing devices.

1 Introduction

Aerodynamics and structural mechanics are two crucial disciplines in the design phase of aeronautical components. They are highly coupled, and their interaction becomes even more relevant in the design of morphing aeronautical structures.

The morphing surfaces or shape adaptation is a concept deriving from the observation of nature [1]. Birds and insects are able to change their wing shape according to a wide range of flight conditions. Similarly, morphing aeronautical surfaces bring numerous advantages compared to rigid conventional solutions. For example, morphing aeronautical engine blades are able to modify their shape according to the aerodynamic requirements at the given operating condition [2, 3, 4], thereby leading to an increase of aerodynamic efficiency and a potential reduction in fuel consumption. The design of such blades is very challenging due to the importance of considering and satisfying contrasting requirements imposed by the two above mentioned disciplines: structural mechanics and aerodynamics. On one hand the structure has to be stiff enough to withstand the aerodynamic loads while maintaining the prescribed aerodynamic properties; on the other hand, it has to be compliant enough to allow shape changes. The result is a compromise between the two requirements. Moreover, aerodynamics and structural mechanics are highly coupled in the design of aeronautical components; therefore, it is highly important to insert in the design process a methodology able to link these two disciplines together. For this purpose, several fluid-structure interaction (FSI) tools have been developed to achieve more complete and reliable results in the design process of morphing structures.

Based on [5], aeroelastic problems can be solved with a classical iterative architecture with coupled aerodynamic and structural models. Indeed, the aerodynamic loads need to be transferred to the structural solver that requires a complete description of the force field to provide an accurate geometry deformation. Conversely, the geometry shape affects the aerodynamics and therefore the computed pressure field by the computational fluid dynamics (CFD) solver. The process continues until it reaches the convergence.

Another example of aero-structure coupling is given in [6] where helicopter rotor airloads are calculated across a range of flight conditions. The coupling between CFD and rotorcraft comprehensive codes can be accomplished in two ways: weak or strong coupling. In the weak procedure, information between CFD and computational structural dynamics (CSD) is transferred on a per-revolution basis; in the strong coupling approach, the CFD and CSD codes are coupled at every time-step and integrated simultaneously.

An FSI method developed in [7] consists in an efficient and robust grid deformation technique, an accurate data interpolation to transfer information from CFD to structural mesh grids and vice-versa, as well as the implementation of suitable interfaces between CFD and structural analysis solvers. The authors demonstrate the significant impact that the FSI has on the aerodynamic analysis and design of transport and combat aircraft.

Another example of FSI is presented in [8], where an aerodynamic shape optimization code is coupled with a structural morphing model in order to obtain a set of optimal wing shapes for minimum drag at different flight speeds. For a given flight condition and aircraft weight, the aerodynamic optimization tool finds the optimal wing shape that is passed to the structural model together with the aerodynamic loads. Then, the process becomes iterative: the structural control points are made coincident to the aerodynamic control points, and the aero loads are distributed to the skin of the structural model; the structural analysis is carried out and the deformation of the skin is obtained. The next iteration consists in passing the new wing shape to an aerodynamic solver and new loads are computed. The process stops when the convergence is achieved.

A multidisciplinary aeroelastic analysis tool for morphing airfoils is described in [9]. This

approach presents some key aspects like the concurrent optimization of aerodynamic and structural parameters of the airfoil, and the ability to consider the static aeroelastic coupling in the analysis of its behavior. In the FSI presented in [9], the pressure on the airfoil surface is transformed into forces acting on the nodes delimiting each structural panel; the aerodynamic model shape is updated by moving the aerodynamic nodes according to the displacements of the neighboring structural nodes resulting from the finite element (FE) analysis. In such a way, the structural and the aerodynamic models are not forced to be based on the same nodes but they can have different levels of refinement.

Another work [10] develops a design method for a 3D morphing wing on an optimization process of structural and aerodynamic design variables. The aeroelastic coupling presented in [10] evaluates the pressure distribution of each wing section by using XFOIL and then, it linearly interpolates them to find the pressure over the whole wing. This information is used for the coupling where the aerodynamic pressure is integrated on each element of the FE model describing the skin of the wing, and each resulting force vector is subdivided on the nodes of the corresponding structural element. Once the FE model of the wing is analyzed, the resulting displacements caused by both actuation and aero-loads define the new aerodynamic shape of the wing. The loop is repeated until convergence.

All the works described above study pure 3D or 2D morphing problems; this means that the same geometry is used for both structural and aerodynamic models. However, there are some situations where it is necessary to couple a two-dimensional problem with a three-dimensional one, and therefore, two different geometries are required. Such a situation usually happens in the preliminary analysis of a complex study like the aero-structural analysis of aeronautical engine blades, where the choice of considering a 2D aerodynamic problem has the purpose of simplifying the process and reducing the computational cost. On the other hand, this assumption makes the aero-structure coupling more challenging because it requires the development of a specific method to match the two-dimensional CFD grid with the three-dimensional finite element analysis (FEA) mesh. Such a mesh matching phase is necessary in order to transfer the aerodynamic loads from the CFD analysis to the structural one. In the present work, a 2D-3D FSI approach is developed and applied to the performance study of a morphing blade cascade.

2 2D-3D Fluid-Structure Interaction Tool

The present work describes step-by-step the developed 2D-3D fluid-structure interaction approach; the proposed FSI tool is employed for a preliminary analysis of the performance of a morphing blade cascade. As mentioned before, the focus of this work is on the 2D-3D FSI tool, therefore, the applied problem has been kept as simple as possible by making assumptions and simplifications as the following: neglecting tip vortices, considering the aerodynamic loads uniformly distributed on the blade, and as already said, a two-dimensional CFD analysis to reduce the computational cost and the complexity of the problem. The final objective of the applied problem is to improve the cascade performance by changing the blade inlet metal angle.

2.1 Applied Problem: Morphing Blade Cascade

As mentioned before, the 2D-3D FSI tool is applied to the preliminary performance analysis of a morphing cascade. The final objective of this analysis is to improve the cascade performance

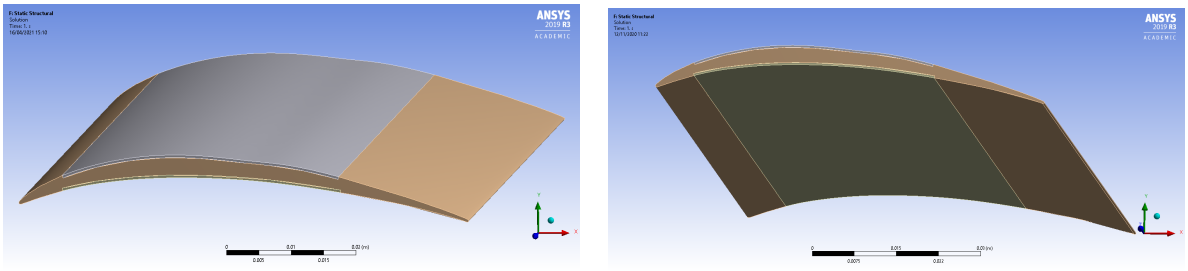

(a) Upper side (b) Lower side

Figure 1: Blade with actuators on the upper and lower sides.

(a) Active actuator on the blade suction side (b) Active actuator on the blade pressure side

Figure 2: Blade morphing due to active actuators.

by changing the inlet metal angle of the blade according to the inflow conditions. To do so, the blade leading-edge geometry is morphed by using two actuators placed on the upper and lower sides of the blade (Fig.1). Once activated, they modify the leading-edge shape by bending the blade upwards or downwards in order to adjust the blade inlet metal angle (Fig.2) leading to a change in the flow conditions, thereby resulting in a possible performance enhancement. In the specific problem presented in this work, the inflow conditions are similar to the one shown in Fig.3; therefore, only the actuator on the pressure side of the blade will be activated in order to move the leading-edge downwards.

2.2 Fluid-Structure Interaction Steps

A schematic representation of the fluid-structure interaction tool is shown in Fig.4. Most of the process is developed by using Ansys Workbench®: geometry generation (SpaceClaim), CFD analysis (Fluent), and finite element analysis (Workbench-Static Structural). Ansys Workbench®has an FSI tool integrated in the software but unfortunately it works with pure 2D or 3D problems. For this reason, it has been necessary to develop a Matlab®script in order to couple the 2D CFD solver with the 3D FEA which is represented by the “Mesh Match” block of the scheme in Fig.4. As described in the following sections, this block is crucial to transfer the aerodynamic loads from the CFD analysis to the structural model.

As shown in Fig.4, the first step is the geometry generation of the 3D baseline blade with the two actuators by using SpaceClaim®. From the mid-span section of the 3D baseline blade, the

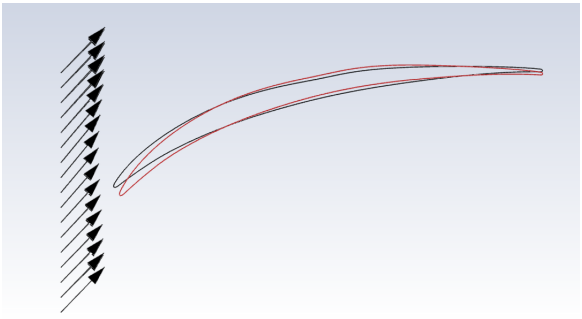

Figure 3: Baseline and morphed blade geometries

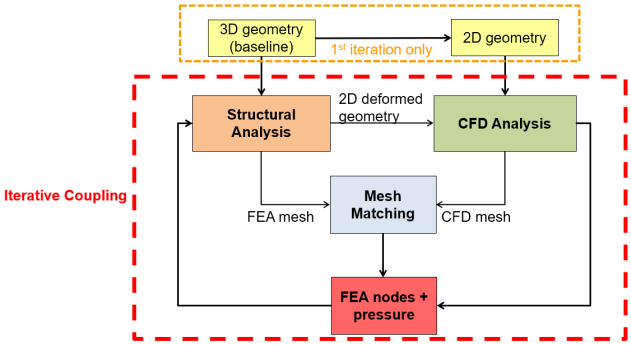

Figure 4: Scheme of the 2D-3D fluid-structure interaction tool

corresponding 2D airfoil geometry is extrapolated and used for the aerodynamic analysis. All the following steps are part of the iterative aero-structure coupling process (Fig.4). As mentioned before, the "Mesh Matching" block is the key element in the FSI framework, and it is the most challenging part of the whole process. In this block, the Matlab code takes the 3D structural mesh nodes coming from the finite element analysis and matches them with the 2D CFD mesh nodes. This matching is important to transfer the aerodynamic loads associated to the CFD mesh nodes to the structural ones. Once the mesh matching is completed, the "matched" FEA nodes with the associated aero-loads are used to run a new structural analysis that returns the deformed blade geometry and the new mesh as output. As shown in Fig.4, the steps in the iterative loop are repeated until a convergence criterion is satisfied. In the following sections, the coupling strategy is explained with more details.

2.2.1 Geometry

The first step is the geometry generation by using Ansys SpaceClaim®. First, the 3D baseline blade is generated. It is a straight blade with no twist, and with an airfoil chord of 70 mm and a span of 120 mm. Two actuators with a thickness of 0.4 mm are used to morph the blade leading-edge, and they are placed one on the pressure side and the other on the suction side of the blade. From the mid-span section of the 3D baseline blade, the corresponding 2D airfoil shape is extrapolated and used in the CFD analysis. The cascade solidity s/c is 0.55, where s

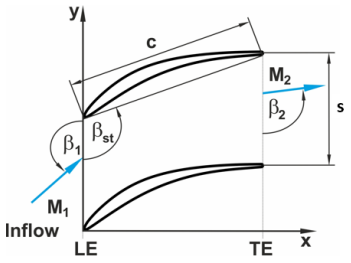

Figure 5: Airfoil cascade

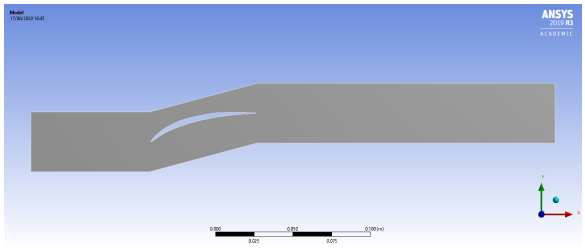

Figure 6: 2D geometry with fluid domain

is the cascade pitch and c is the chord length (Fig.5), and the airfoil is rotated such that the stagger angle β_s is 107.37 deg (Fig.5). Based on that, the fluid domain is drawn considering the inlet at a distance of $2s$ from the leading-edge of the airfoil, and the outlet at $5s$ from the trailing-edge of the airfoil (Fig.6).

2.2.2 Finite Element Analysis

The finite element analysis is conducted in Ansys Workbench®, and a schematic representation of the steps is shown is Fig.7. Block A is the first step where the material properties for the blade and the actuators are listed; in particular, aluminum alloy is assigned to the blade, and shape memory alloy (SMA) to the actuators.

After the material assignment, the 3D blade geometry generated in block C is imported into the blocks B and D where the mesh is generated separately for the blade and the two actuators; block B generates the mesh for the blade without the actuators (Fig.8), while block D models only the two actuators and generate the mesh (Fig.9). It is important to remind the reader that this work is focused on the 2D-3D fluid-structure interaction tool; therefore, the SMA model used in the structural analysis is extremely simplified and a more advanced one will be implemented in future works. For this reason, the SMA material is modeled as an isotropic material with linear material behaviors. The martensite and austenite stiffness as well as the hysteresis are not taken into account, and the actuation of the SMA is considered only in one direction. The Young's modulus for the SMA is 30 GPa, and the Poisson's ratio 0.33, since the actuators are modeled in first approximation by assuming that they are made by 100% SMA. For such a simplified SMA model, a thermal analogy is used with a thermal coefficient α of -2%

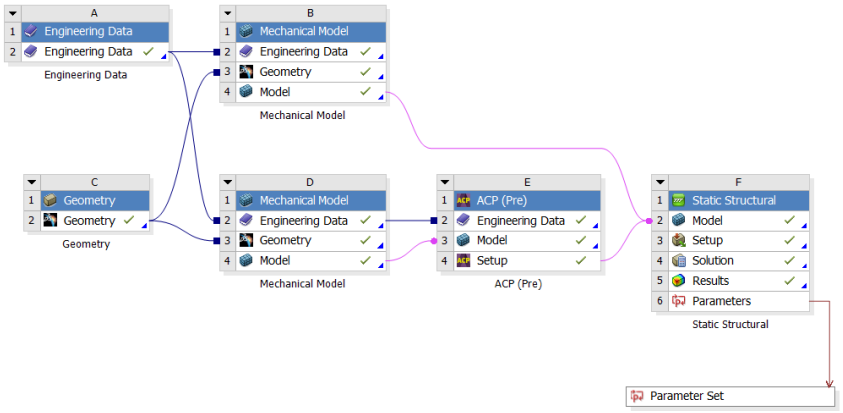

Figure 7: Steps for the structural analysis in Ansys Workbench®

per 100°C temperature difference:

$$\alpha = \frac{\epsilon}{\Delta T} = \frac{-0.02}{100} = -0.0002/^{\circ}C \tag{1}$$

The simplified model for the SMA actuators requires the assignment of a "polarization direction" (block E) that defines the fiber orientation of the material meaning the axis along with the actuators deform when activated. Figure 10 shows that the SMA material is oriented along the x-axis (chordwise direction); this means that once a temperature is assigned to the material, the actuators contract in the x-direction as shown by the arrows in Fig.10. The last step is done in block F where the blade and the actuators are combined together. At this point, the boundary conditions for the structural analysis are defined in terms of edge clamping and thermal condition for the actuators. The blade is clamped on both lateral sides, considering only the area of the blade close to the trailing-edge and not covered by the actuators (Fig.11). In particular remembering that the x-axis is chordwise and the z-axis is spanwise, the three directions x, y, and z are set to zero (clamped) at the coordinate z=0 (blade root); while at z=120 mm (blade tip), the z-direction is left free not to over-constrain the blade and to avoid unwanted internal stresses. Another important parameter to set for the actuators is the thermal condition, which is the temperature that based on the thermal analogy simulates the voltage on the actuator that leads to its activation. For the present work, the value assigned to the thermal condition is 100°C for the active actuator (Fig.12), considering that 0°C corresponds to zero strain. As mentioned before based on the inflow conditions, the active actuator considered in this work is the one on the blade pressure side; therefore, the thermal condition is applied only to the actuator at the bottom of the blade.

2.2.3 Computational Fluid Dynamic Analysis

The CFD analysis is conducted in Ansys Fluent®. As mentioned in Sec.2, a 2D analysis is considered (airfoil cascade) in order to reduce the computational cost and the complexity of the problem. One single airfoil is simulated and the baseline geometry is extrapolated from the mid-span section of the whole 3D baseline blade (Sec.2.2.1). The inflow conditions are characterized

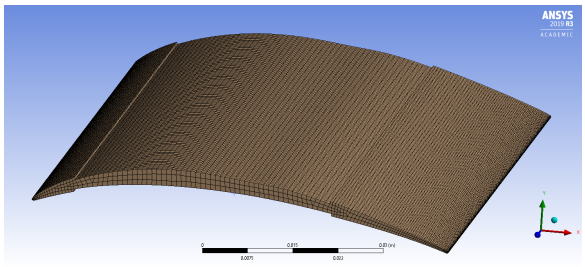

Figure 8: Mesh of the blade without the actuators

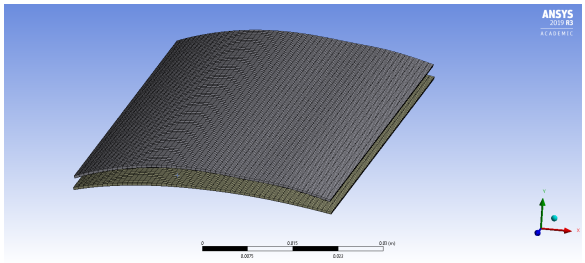

Figure 9: Mesh of the two actuators

by the inlet Mach number of 0.61, the inflow angle β_1 of 138 deg (off-design), the inlet total temperature is 315 K, and the inlet total pressure is 122500 Pa.

Figure 13 shows the steps followed in the aerodynamic analysis. The 2D mesh generated by using the Ansys mesher tool is quadrilateral with 30 prism layers close to the airfoil surface in order to have a $y+ \leq 1$. After a grid independence study, the final mesh has about 150000 elements (Fig.14), and it takes only few seconds to be generated.

The boundary conditions assigned to the fluid domain are represented in Fig.15: the airfoil is a no-slip wall, the inlet is a pressure inlet, and the outlet is a pressure outlet. The two sides above and below the airfoil are periodic boundaries to simulate the cascade.

The flow is steady, compressible and fully turbulent; the $k-\omega$ shear stress transport (SST) turbulence model is selected and coupled with a $y+ \leq 1$ close to the airfoil surface such that the entire boundary layer can be solved. The computational time for a single CFD simulation is about 10 min by using four processors in parallel. For reliable results, a validation of the CFD results is necessary and it has been done in [11].

2.2.4 Mesh Matching

As already mentioned, the mesh matching step is the most important in the FSI process presented in this article. The main difficulty is to build a tool able to match the 3D FEA mesh with the 2D CFD one. Figure 16 shows the FSI steps described so far; no aerodynamic loads are transferred yet, and the geometry is the baseline without any deformation.

At this point, the “Mesh Matching” box takes the 3D structural mesh and the 2D CFD mesh as input, and it returns the 2D FEA mesh nodes with the associated static pressure resulting from the CFD analysis. In particular, the structural mesh nodes represented in Fig.17

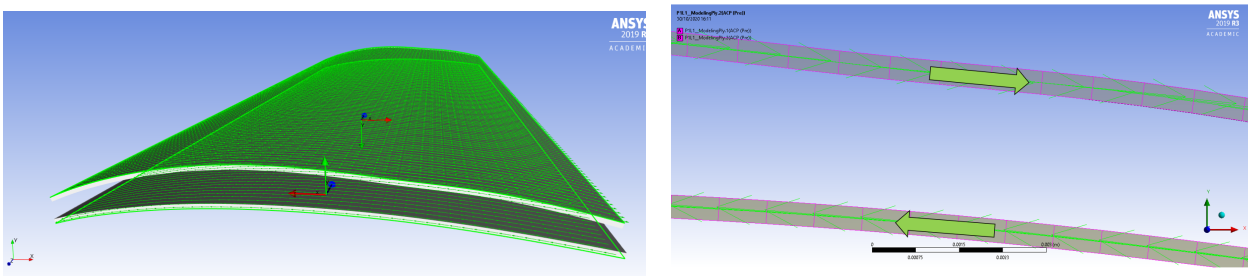

(a) (b)

Figure 10: Direction of deformation for the two SMA actuators.

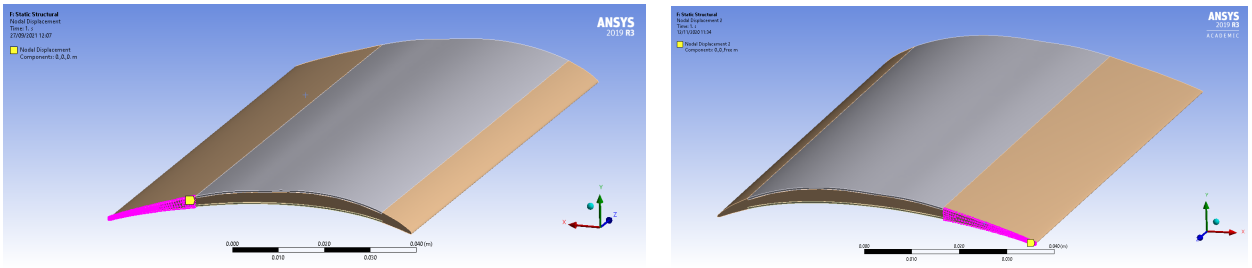

(a) Blade root (b) Blade tip

Figure 11: Clamped area at the lateral sides of the blade.

are filtered in order to select only the mid-span section nodes. At this point, another filtering process is necessary to get only the structural mesh nodes on the surface of the mid-span section (airfoil) in order to compare them with the 2D CFD nodes (Fig.18). The distance between the 2D coordinates of the filtered FEA nodes and the CFD ones is calculated, and the closest CFD nodes to the filtered FEA nodes are found. Now, it is possible to transfer the static pressure originally associated to the CFD nodes to the 2D filtered FEA nodes. Therefore, the output of the "Mesh Matching" phase is given by the x and y-coordinates of the filtered FEA nodes and the associated static pressure (Fig.19). Once the matching phase is completed, the aero-loads can be easily transfer to the structural analysis for a new run (Fig.20).

2.2.5 Finite Element Analysis with Aero-loads

As mentioned in Sec.2.2.4, the aerodynamic loads can be transferred to the structural analysis, and a new run can start considering now the effects of aero-loads and activation of the actuator. To import the static pressure associated to the 2D filtered FEA mesh, the "External Data" tool in Ansys Workbench®is used (Fig.21). There, it is possible to upload a data table with the x and y-coordinates of the mesh nodes and the static pressure associated to them. Once the "External Data" block is linked to the the "Static Structural" one, it is possible to visualize the transferred aero-loads on the 3D blade in the finite element analysis. The pressure distribution on the blade mid-span section coming from the CFD is projected over the whole 3D blade span (Fig.22). It is well known that this is not a realistic approximation but it is necessary to keep

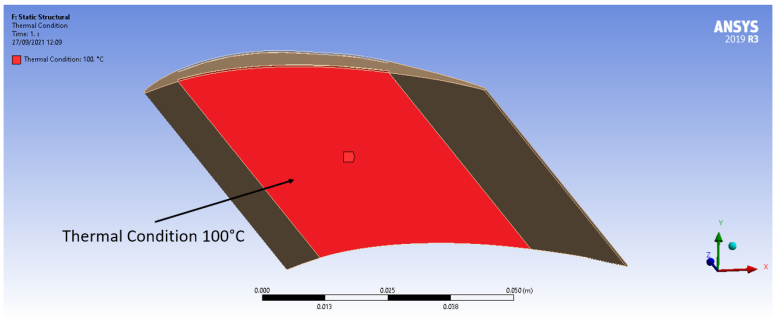

Figure 12: Thermal condition applied to the lower side actuator.

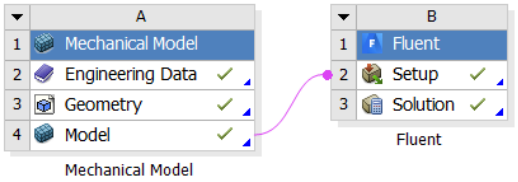

Figure 13: Schematic representation of the steps for the CFD analysis.

the problem as simple as possible since the main focus of this work is on the FSI tool.

Once the aerodynamic loads are uploaded into the structural analysis, the actuator on the pressure side of the blade is activated and the resulting deformed geometry due to both aero-loads and actuation is found (Fig.23). From the 3D deformed shape, it is possible to extrapolate again the corresponding 2D deformed geometry that is passed to the successive CFD analysis.

The steps described in the previous and present sections are repeated in an iterative loop until convergence. The aero-structure coupling stops when the convergence criterion is satisfied meaning when the difference in the leading-edge displacement along the y-axis (Fig.23) between two consecutive iterations is less than a given tolerance value.

3 2D-3D FSI Tool Application and Results

The iterative FSI process described in the previous sections has been applied to four morphing blade configurations with different actuator dimensions and position (Fig.24). The aero-structure coupling stops when the difference in the leading-edge displacement along the y-axis between to consecutive iterations is less than $2 \cdot 10^{-5}$ [m]:

$$\Delta y = y_i - y_{i-1} < 2 \cdot 10^{-5} \tag{2}$$

Figure 25 shows the value of Δy as function of the iteration counter for the four blade configurations. As it is possible to notice, all the simulated cases show a convergence after up to four iterations.

Once the convergence of the FSI framework has been empirically proved, it is interesting to

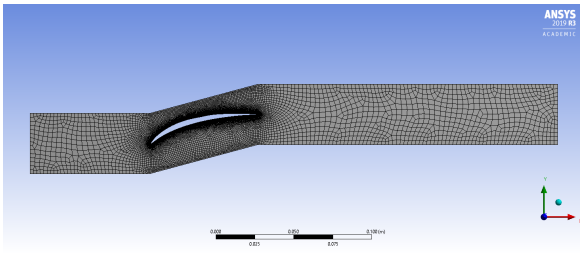

(a) CFD mesh

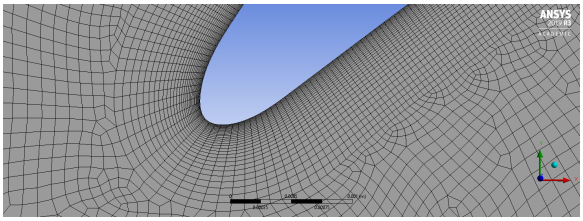

(b) Mesh at the leding-edge

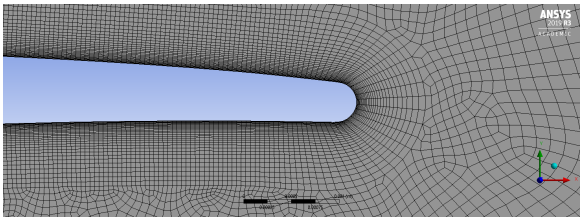

(c) Mesh at the trailing-edge

Figure 14: CFD mesh with detailed view on the leading and trailing edges.

see how the resulting deformation at the leading-edge affects the cascade performance in terms of total pressure loss coefficient ω:

$$\omega = \frac{p_{01} - \bar{p}_{02}}{q_1} \tag{3}$$

where p_{01} is total pressure at inlet, $\bar{p}_{02}$ is the average total pressure at outlet, and q_1 is the dynamic pressure at inlet. A reduction of ω means a reduction in the pressure losses, and therefore, an enhancement in the cascade aerodynamic performance. Before showing the results, it is important to remind that the blades are working in off-design conditions ($\beta_1 = 138$ deg), and therefore, the flow over the airfoil is characterized by a strong separation that is mitigated significantly thanks to the leading-edge morphing, as shown in Fig.26.

Table 1 summarizes the results in terms of total pressure loss reduction, y-displacement at the leading-edge, and inlet blade metal angle (κ_1) for the four blade considered. It is possible to notice that the four morphing blades show a reduction in the total pressure losses up to 53% thanks to a leading-edge displacement between 0.6-1.5 mm in the downward direction that significantly affect the blade inlet metal angle.

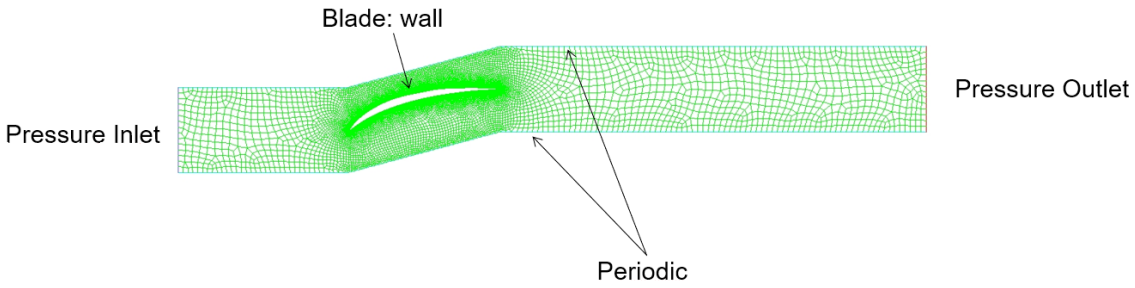

Figure 15: CFD boundary conditions.

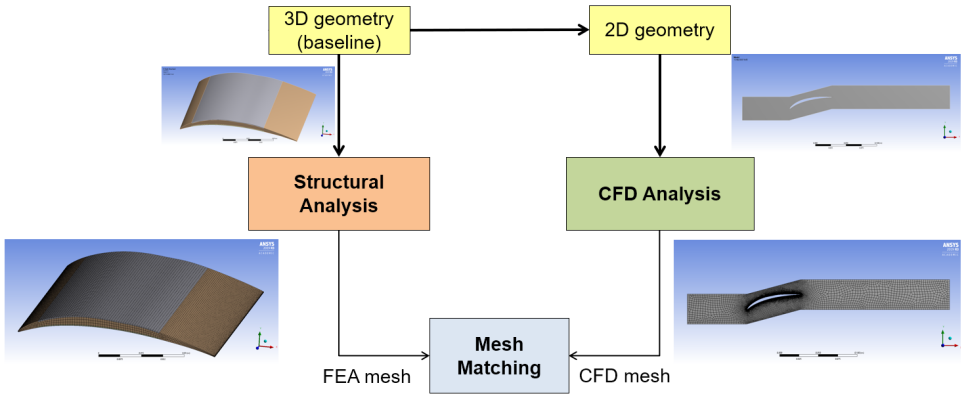

Figure 16: FSI scheme at the first stage when no aerodynamic loads are involved.

Table 1: Results

Blade	Total P loss reduction [%]	y-displacement [m]	κ_1
Baseline	-	-	46.88
Case 1	53	-0.00146	51.04
Case 2	50	-0.00138	50.83
Case 3	49	-0.00104	49.86
Case 4	50	-0.00059	48.57

4 Conclusion

The work presented in this paper focuses on the development of a 2D-3D fluid-structure interaction framework where a two-dimensional CFD analysis is coupled with a three-dimensional structural model. The developed FSI tool is also applied to a simplified problem in order to highlight the reliability of the method. In particular, the performance of a morphing airfoil cascade has been studied and the results in terms of total pressure losses, leading-edge displacement, and inlet metal angle have been analyzed. By applying the 2D-3D FSI tool at four different

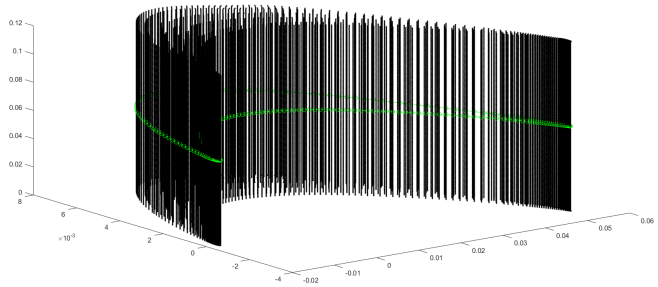

Figure 17: Mesh nodes of the whole 3D blade.

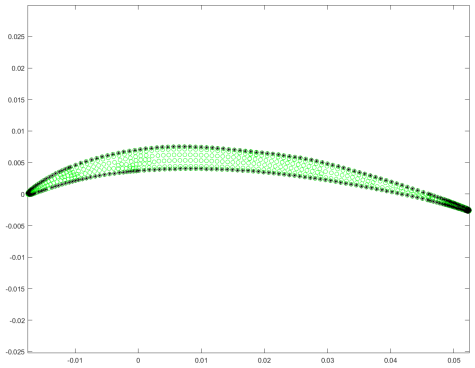

Figure 18: Mesh nodes of the mid-span section.

blade configurations, it is possible to notice that the iterative process stops after three iterations for the first three blades and after four iterations for the last blade considered. Moreover, the FSI approach gives consistent results in terms of cascade performance for all the four simulated blades with an reduction in the total pressure losses up to 53%.

REFERENCES

[1] Vincent, J.F.V. *Smart by name, smart by nature.* (2000) Smart Materials and Structures 9.

[2] Mueller, T. and Lawerenz, M. *Shape adaptive airfoils for turbomachinery applications undergoing large deformations* (2003) 44th AIAA/ASME/ASCE/AHS/ASC Structures, Structural Dynamics, and Material Conference

[3] Riemenschneider, J., Huxdorf, O. and Opitz, S. *Effects of piezoceramic actuator in quasistatic use* (2014) Smar Materials, Adaptive Structures and Intelligent Systems.

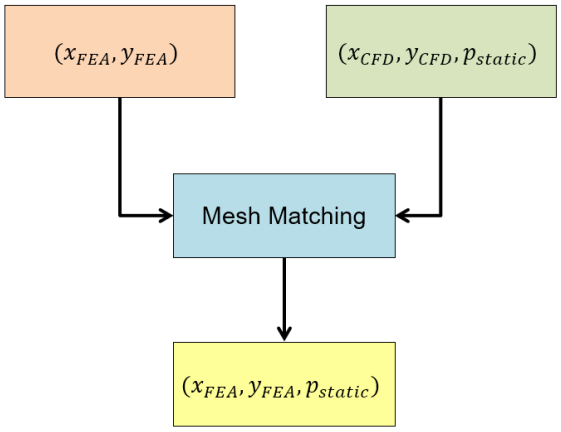

Figure 19: Mesh matching steps.

[4] Monner, H.P., Huxdorf, O., Riemenschneider, J. and Keimer, R. *Design and manufacturing of morphing fan blades for experimental investigations in a cascade wind tunnnel* (2015) 23rd AIAA/AHS Adaptive Structures Conference

[5] Ricci, S. and Terraneo, M. *Application of MDO techniques to the preliminary design of morphed aircraft* (2006) 11th AIAA/ISSMO Multidisciplinary Analysis and Optimization Conference.

[6] Potsdam, M., Yeo, H. and Johnson, W. *Rotor airloads prediction using aerodynamic/structural coupling.* (2006) Journal of Aircraft.

[7] Kroll, N., Heinrich, R,, Krueger, W. and Nagel, B. *Fluid-structure coupling for aerodynamic analysis and design: a DLR perspective.* (2008) 46th AIAA Aerospace Sciences Meeting and Exhibit.

[8] Gamboa, P., Vale, J., Lau, F.J.P. and Suleman, A. *Optimization of a morphing wing based on coupled aerodynamic and structural constraints.* (2009) AIAA Journal.

[9] Molinari, G., Quack, M., Dmitriev, V., Morari, M., Jenny, P. and Ermanni, P. *Aerostructural optimization of morphing airfoils for adaptive wings.* (2011) Journal of Intelligent Material Systems and Structures.

[10] Molinari, G., Arrieta, A.F. and Ermanni, P. *Aero-structural optimization of three-dimensional adaptive wings with embedded smart actuators.* (2014) AIAA Journal.

[11] Abate, G., Riemenschneider, J. and Hergt, A. *Aero-structural coupling strategy for a morphing blade cascade study* (2022) ASME Journal of Turbomachinery.

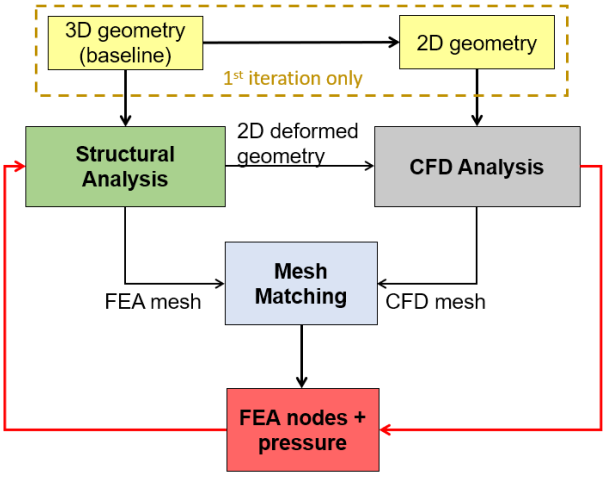

Figure 20: FSI scheme with the aerodynamic loads.

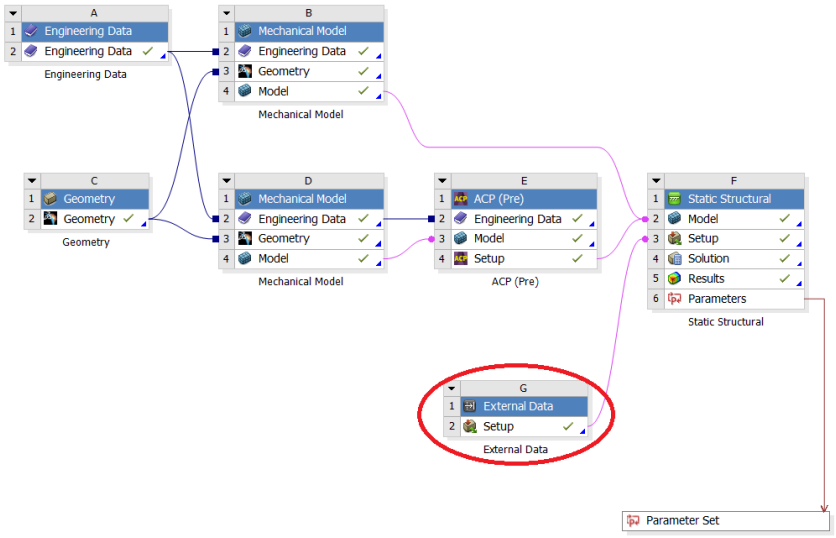

Figure 21: External Data tool for importing the aero-loads.

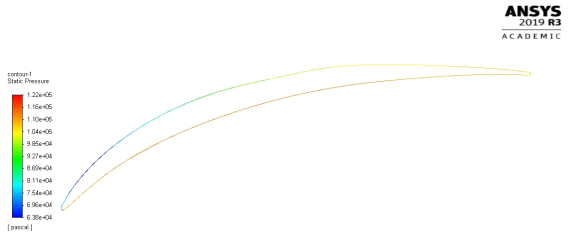

(a) 2D airfoil

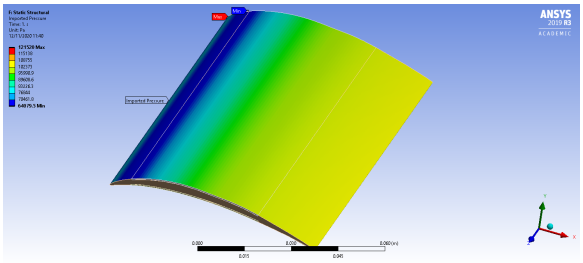

(b) Blade suction side

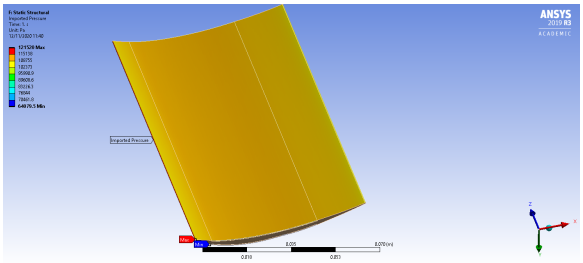

(c) Blade pressure side

Figure 22: Same pressure distribution in the CFD and FEA analyses.

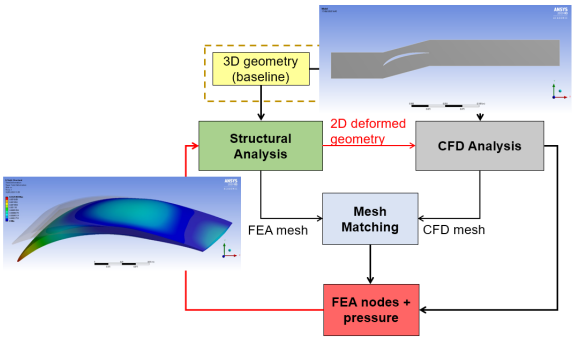

(a) Schematic representation of the structural analysis output

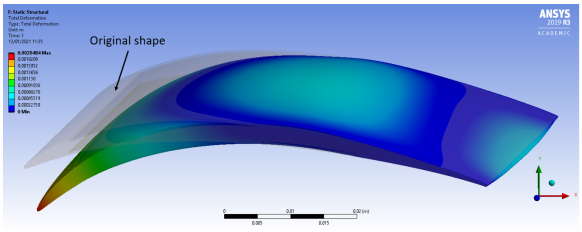

(b) 3D baseline-deformed geometry comparison

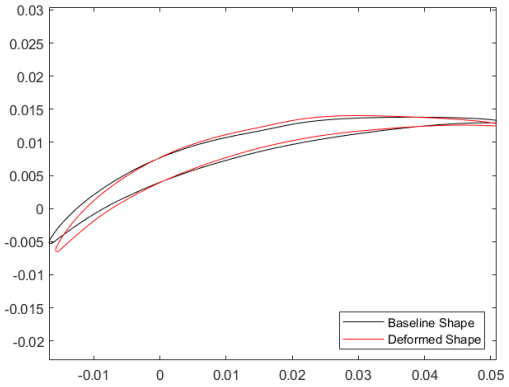

(c) 2D baseline-deformed geometry comparison

Figure 23: Resulting 3D and 2D deformed geometries.

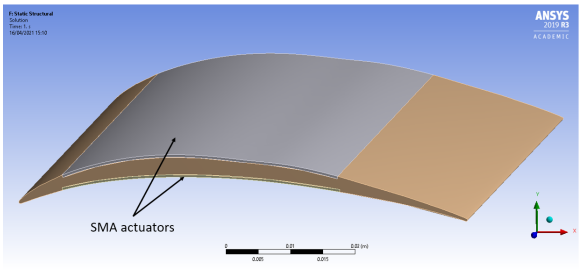

(a) Case 1

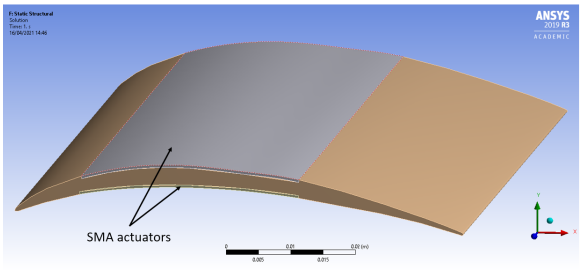

(b) Case 2

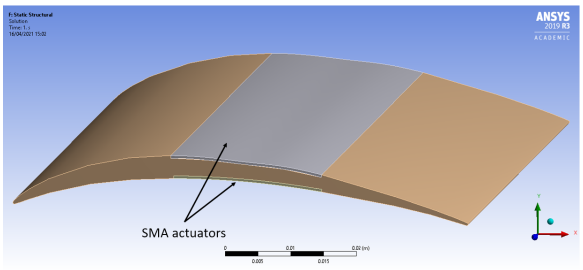

(c) Case 3

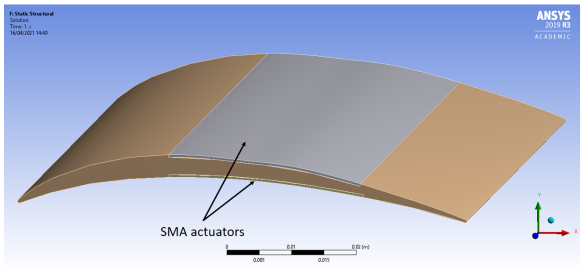

(d) Case 4

Figure 24: Four blade configurations.

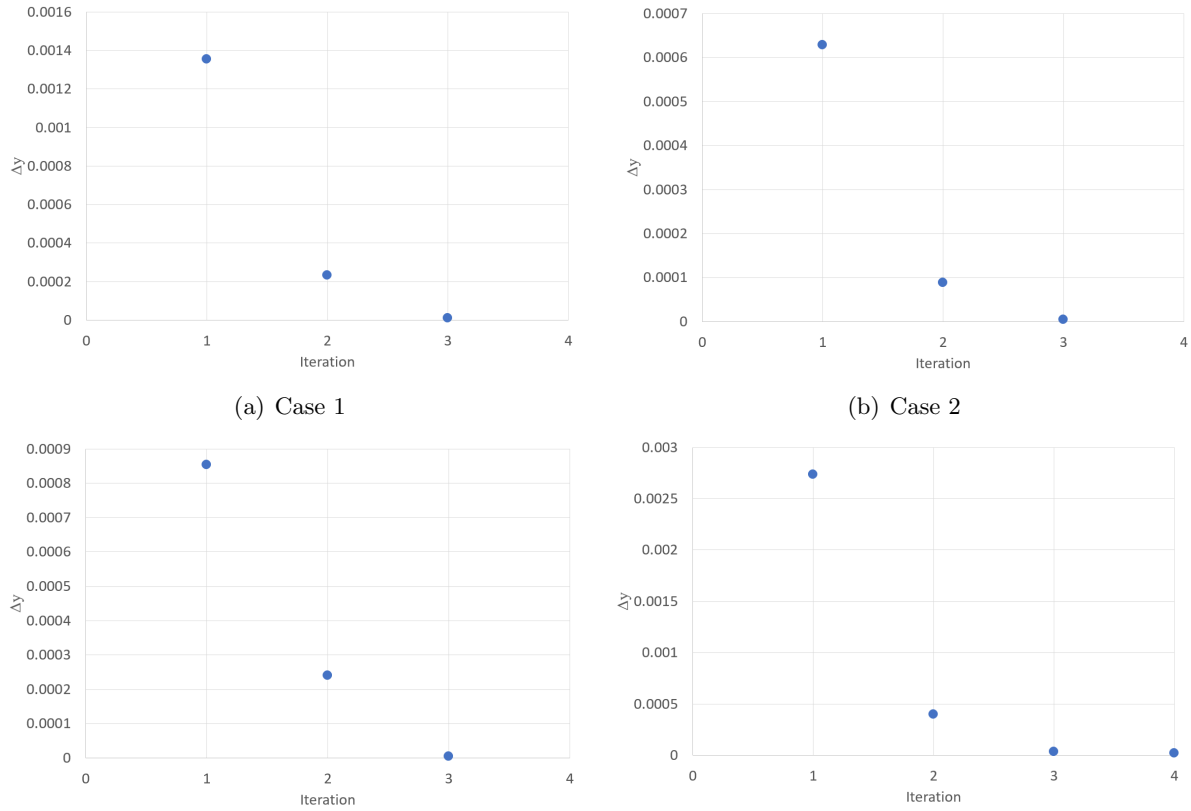

(a) Case 1 (b) Case 2

(c) Case 3 (d) Case 4

Figure 25: Iterations in the FSI loop for the four different blade configurations.

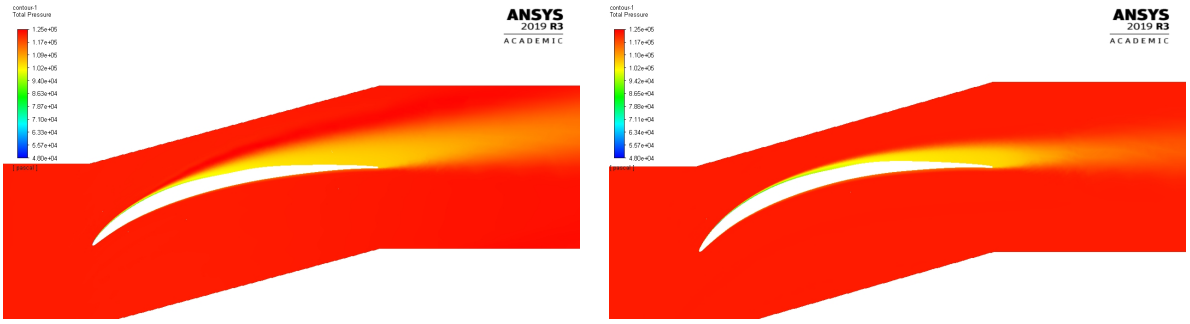

(a) Baseline blade (b) Morphed blade

Figure 26: Total pressure distribution of the baseline blade and a morphed blade (Case 1).